A flexible temperature sensing finger using optical fiber grating for soft robot application*

HE Qing (贺庆) **and ZHANG Qingchao** (张青超)**

School of Instrument Science and Opto-Electronics Engineering, Beijing Information Science and Technology University, Beijing 100192, China

(Received 15 September 2020; Revised 12 November 2020)

Bionic perception, especially temperature-aware, is one of the important issues in soft robots research. This paper presents a method to implant temperature sensor network into soft robot finger by using optical fiber gratings. For avoiding strain disturbance, a dedicated metal tube is designed to package and protect the optical fiber gratings. For implanting the sensors firmly, a solution using two kinds of adhesive is proposed. The prototype is calibrated in high precision temperature bath and then measured under different temperatures and different bending conditions, respectively. The experimental results are compared with electronic temperature sensor (PT100 thermal resistance), which verifies the accuracy and repeatability of the design. With the dedicated coating and adhesive solution, the proposed temperature sensor network is suitable for implanting into soft robots for the temperature-aware ability.

Document code: A **Article ID:** 1673-1905(2021)07-0400-7

DOI https://doi.org/10.1007/s11801-021-0144-0

Recently, soft robot has been a crucial research subfield in robotics[1-3]. Owing to its flexibility, it has wide applications in military, rescue, surgery and so on[4,5]. In the future, the soft robot can have wider application range by integrating sensitive perception, such as temperature sensors, which makes them detect the external world[6].

Temperature sensing is a very practical ability for soft robots since they are usually applied in complex and unpredictable circumstance[7,8]. In some disaster areas, the rescue robot can search for survival according to the body temperature[9]. In surgery, the diagnostic robot can monitor the temperature of different parts of the patient's body. And in nuclear power station, the supervisor robot can early alarm the abnormal environment temperature[10]. More importantly, most of material compositions of soft robots, such as hydrogel, plastics, silicone and rubber, cannot endure excessive temperatures[11,12]. For the purpose of self-protection, temperature-sensing is an essential ability for a robotic system, just like animals.

Different from the rigid robots, soft robots demand the integrated sensors to be bendable and flexible[13]. The rigid or big temperature sensors could be unsuitable[14]. Infrared sensor and acoustic tomography are useful to measure the surface temperature of the object in the distance. Thereby the methods are good supplements to robot vision[15,16]. Nevertheless, they are inappropriate to feel the ambient temperature like animal's skin. The existing temperature sensors for soft robots are mostly realized by the compact electronic sensors, i.e. electro-resistances polymer, thermocouples, composite semiconductor, interdigitated electrode structure, MEMS chips and so on[12,17,18]. However in special occasions, such as high electromagnetic radiation, inflammable gas or underwater, the electronic sensors are difficult to work. And the other sensors designed with new materials have respective advantages but they are in common hard to manufacture[19].

Compared with the traditional sensors, optical fiber Bragg grating (FBG) temperature sensors have the advantages of small size, anti-radiation, and anti-electromagnetic interference. Nowadays, its technology has been widely used in power system, construction, chemical, aerospace, medical and other fields at home and abroad[20]. The application of FBG in robots currently mainly involves in shape perception[21], tactile perception[22,23], strain perception[24] and pressure perception[25]. Although the optical fiber grating has been used as temperature sensor for the other fields[26,27], it has not been applied to the soft robot because the strain resulted from soft robots deformation can affect the temperature measurement of FBG.

In this paper, a temperature sensor network using optical FBG is proposed for soft robot finger. By virtue of its slim and bendable characteristics, optical fiber grating has developed into a mature technology with a broad range of applications in various areas[28,29]. Due to the strain and temperature can both affect the return wavelengths of FBG, a dedicated steel tube is designed to

* This work has been supported by the National Natural Science Foundation of China (No.51775051), and the Scientific Research Project of Beijing Educational Committee (Nos.KM201911232019 and KM202011232008).

** E-mail: Will@mail.bistu.edu.cn

package the FBG and the packaging technology are described in detail. On the other side, two kinds of adhesive are applied to stick the optical fiber with soft robot firmly. The layout of the steel tubes has been carefully arranged so that the sensors can match up with the action of bending and grasping of soft robot finger. Then the sensors are calibrated in high precision temperature bath. For verification, several experiments are implemented under different temperatures and different curvature. The measured results of the temperature-sensing finger are in good agreement with the high precision thermometer, which demonstrates the accuracy and feasibility of the proposed design. Better than the electronic sensors, optical fiber sensors have immunity to the issue of electromagnetic interference (EMI) intrinsically and can work under water[30]. As a relatively mature temperature sensing solution, it can solve the temperature sensors problems of software robots.

The working mechanism of optical fiber can be divided into three basic categories: intensity-modulated, phase-modulated, and wavelength-modulated. In this paper, the temperature sensing finger is designed based on wavelength-modulated optical fiber gratings. According to Bragg conditions, we obtain

$$\lambda_B=2n_{eff}\cdot\Lambda, \tag{1}$$

where n_{eff} and Λ denote the effective refractive index and grating period of the FBG, respectively. Ambient temperature affects the variation of n_{eff} and Λ by thermal-optic effect and thermal-expansion effect. Take the derivative of both sides with respect to temperature T, we can get the following equation:

$$\frac{1}{\lambda_B}\frac{d\lambda_B}{dT}=\frac{1}{n_{eff}}\frac{dn_{eff}}{dT}+\frac{1}{\Lambda}\frac{d\Lambda}{dT}. \tag{2}$$

The first term on the right side which is related to the thermal-optic effect is defined as thermal-optic coefficient. And the second term which is related to the thermal-expansion effect is called as thermal expansion coefficient. Thus after calibration, we can obtain the corresponding temperature with the shift of Bragg wavelength λ_B. Because thermal-expansion effect and the thermal-optic effect work instantaneously, the FBG can be seen as a real-time sensor.

On the other hand, external influence, such as vibration and strain, would also cause the shift of Bragg wavelength λ_B. Compared with rigid robots, soft ones tend to suffer from external influence. Therefore, the sensors should be carefully packaged and embedded in the soft finger appropriately. The model photograph of this design is shown in Fig.1 and the fabrication procedure is as follows.

Firstly, we design a slender tube which is made by stainless steel (SUS 304) to protect the FBG. The steel tube cannot be too thick to hinder the bending of soft finger. Penetrate the optical fiber into a stainless steel tube and make sure that the part of FBG is located in the middle of the steel tube. During the packing process, the optical fiber is imposed to a slight radian without touching the shell of tube so that the inside optical fiber remains a slack status no matter how the steel tube is stretched or compressed.

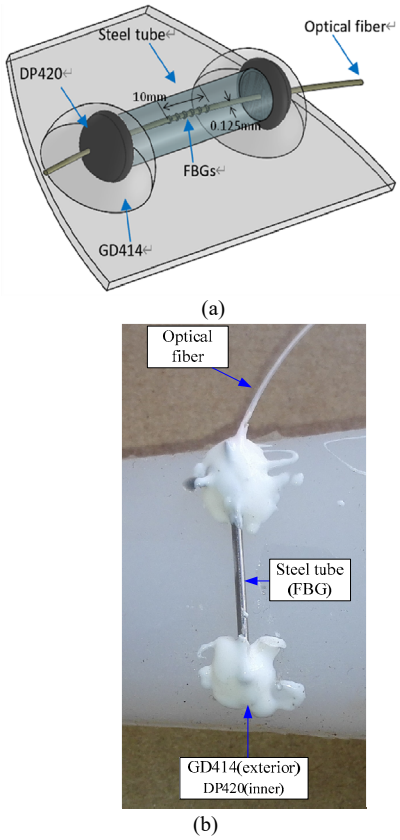

Fig.1 The optical fiber temperature sensor integrated in the soft finger: (a) 3D schematic; (b) Photograph of the prototype

The main material of the usual optical fiber is SiO_2 and its surface is smooth so that it is hard to stick the optical fiber with soft robot which is mainly made up of rubber. For solving this problem, two kinds of adhesives are used. Firstly fix and paste the two ends of steel tube with optical fiber using the 3M DP420, an epoxy adhesive, until the structure is solidified. DP420 is a high efficient adhesive which has been applied to stick optical fiber with satellite, wing, and bridge. It can avoid the creep of optical fiber caused by strain or temperature.

Although the DP420 can stick optical fiber with rigid ones together firmly, it can't stick on the silicon rubber material what we adopt as the soft finger substrate. Therefore, we use another adhesive GD414, a dealcoholization vulcanization silicon, to stick two solidified DP420 ends with the silicon rubber substrate, as shown in Fig.1. The two adhesives ensure the fastness and repeatability of the sensors. For avoiding hindering the action of the finger bending, the steel tube is laid vertical to the movement orientation of the finger.

Thus, the sensor could be integrated in the soft robot finger firmly and wouldn't restrict the movement and

bending of the finger. For monitoring the temperature of different position, we can align these sensors along the lengthways.

The proposed soft robot finger whose shape is like Octopus hand is made by Smooth-on Ecoflex 0050 silicon rubber. The optical fibers we adopt are single-mode ones with the effective refractive index of 1.447. For monitoring the temperatures of different parts of finger, there are seven optical fiber sensors aligned along the lengthways while each sensor is laid along the horizontal, just as Fig.2. The sensors from top to bottom are named after sensor1 to sensor7. The FBGs whose specific parameters are listed in Tab.1 are adopt as the sensor units.

Since the optical fiber is doped with element Ge in the process of manufacture, the temperature sensitivity of real FBG is different from the theoretical value. Consequently, to determine the temperature profile of the sensor network, it is necessary to calibrate their temperature coefficient which reflects the relationship between the Bragg wavelength shift and temperature variation.

The instrument used for calibration is the Fluke 7381 high precision bath which is well-known for excellent temperature control that maintains excellent temperature stability (±0.005 °C) and uniformity (±0.007 °C). Because there is a forceful water-flow when the bath works, the soft robot finger must be firmed with lead screws and bracket, which is shown in Fig.2. The calibration temperature range is set from 10° to 65°, which is the normal working temperature range of the finger (the silicon is prone to aging and deformation in high temperature). Before each temperature point measurement, the temperature of water keeps constant for 10 min to assure thermal equilibrium between the finger and the water. Then the signals on temperature are demodulated by an FBG demodulator with 1 pm wavelength resolution. The measurement variation of wavelength shift on temperature is illustrated in Fig.3.

From the calibration curves of the FBG sensors, the mapping relationships between temperature and wavelength can be fit to the following equations in which the subscript n expresses the serial number of the sensors, λ_n presents the current wavelength of every sensor and Tem_n stands for the temperature measured by the sensors. k_n and b_n mean the fitting coefficients, which are calculated and listed in Tab.2.

$$Tem_n=k_n\cdot\lambda_n+b_n. \tag{3}$$

The linearity and accuracy of the sensors can be calculated by the statistical analysis of the dispersion of the temperature measurements, i.e. taking the R-square and standard deviation of the measurement results. Tab.2 shows the R-square and standard deviation (σ) of every sensor. The theoretic resolution of every sensor is about 0.1 °C which depends on the resolution of demodulator. Afterwards, according to the reflected wavelength of FBGs, the ambient temperature may be obtained.

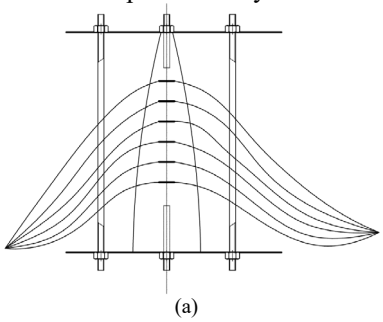

(a)

(b)

Fig.2 The firmed soft robot finger for calibration: (a) Schematic diagram; (b) Photograph (sensor 1 to 7 named from top to bottom)

Tab.1 Parameters of the FBGs

Parameters	Values
Central wavelength	1 530 nm, 1 534 nm, 1 538 nm, 1 540 nm, 1 544 nm, 1 548 nm, 1 559 nm
Length of grating region	10 mm
3 dB bandwidth	≤0.01 nm
Reflectivity	≥90%
Refractive index	1.447

The results show that the wavelengths of the sensors shift significantly toward the higher wavelengths with the rising of temperature. This phenomenon can be explained by thermal-optic effect and thermal-expansion effect. Experimental results of most sensors reveal an approximate linear relationship between wavelength and temperature within the working range, as expected. However, it also can be observed that the standard deviations of sensor5 and 6 are above 1 °C and the R-squares are worse than the others obviously. The possible reason

is that the FBGs don't remain a proper radian or directly contact with the inner sheath of the steel tube when it is packaged. Steel has high temperature sensitivity because thermal expansion coefficient of metal is much greater than that of optical fiber. Thus when the temperature rises, the FBG is stretched by the steel tube so that the shift of wavelength is affected by the expansion of the steel tube. While the temperature drops, the optical fiber becomes loose and the shift of wavelength is mainly decided by its own Bragg condition. Therefore the two non-linear sensors which have standard deviation above 1 °C can not be useful for the temperature measurement. For measurement accuracy, they are ignored in the following experiments.

Tab.2 The parameters of calibration fitting lines of the sensors

Parameters	Sensor1	Sensor2	Sensor3	Sensor4	Sensor5	Sensor6	Sensor7
k_n	97.977 71	105.087 64	102.258 06	106.090 49	57.217 06	73.404 77	85.660 61
b_n	-152 818.1	-161 629.9	-157 491.0	-162 371.2	-88 573.5	-112 601.7	-132 291.6
R-square	0.999 6	0.999 4	0.997 3	0.998 8	0.990 2	0.989	0.999 4
σ	0.324 7 °C	0.437 8 °C	0.786 6 °C	0.475 4 °C	1.556 °C	1.425 °C	0.363 3 °C
Resolution	0.1 °C	0.1 °C	0.1 °C	0.1 °C	0.1 °C	0.1 °C	0.1 °C

For verifying the validity of the sensor network, the sensors are measured and compared with the electronic thermometer. The applied electronic thermometer is AZ 8821 which employs the PT100 as sensitive element and has the resolution of 0.01 °C and precision of ±0.2 °C. Its temperature result serves as a reference to verify the measured data of the proposed prototype.

First, the prototype is measured in the room, in which the temperature is controlled by air control and the range is from 16.63 °C to 24.14 °C. In the range, we choose 6 different temperature points and record the wavelength shift for 15 min at every temperature point. The measurement results are listed in the Tab.3. According to the data of Tab.3, the measured temperatures compared with the thermometer are plotted in Fig.4.

From the figure, we find the uniformity of the sensors is well and the sensors network can distinguish tiny temperature variation. The temperature differences between the sensors and the electronic thermometer are all below 1 °C. So the soft finger can monitor the temperature instead of the electronic thermometer in the measured range.

Tab.3 The wavelength measurement results against the thermometer in the room

Thermometer (°C)	Sensor1 (nm)	Sensor2 (nm)	Sensor3 (nm)	Sensor4 (nm)	Sensor7 (nm)
16.63	1 559.900	1 538.210	1 540.304	1 530.658	1 544.567
18.92	1 559.921	1 538.227	1 540.323	1 530.676	1 544.590
20.33	1 559.935	1 538.241	1 540.335	1 530.690	1 544.606
21.55	1 559.941	1 538.250	1 540.343	1 530.695	1 544.615
22.56	1 559.952	1 538.260	1 540.356	1 530.706	1 544.631
24.14	1 559.973	1 538.282	1 540.376	1 530.726	1 544.654

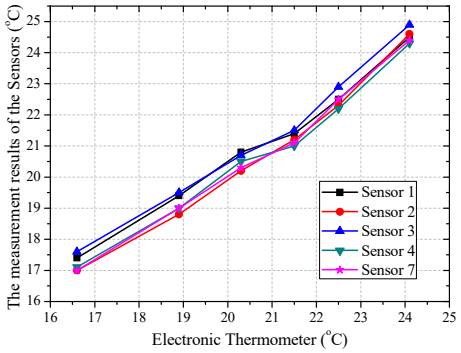

Fig.4 The corresponding measured temperatures with both the electronic thermometer and the sensors

The main difference between soft robot and rigid robot lies in whether the limbs can bend at any degree of freedom. For analyzing the influence of finger curvature, we design a steel plate with many camber grooves of different curvature. Using the steel plate, three iron sheets are made with the representative curvatures of 8.7 m^{-1}, 6.3 m^{-1} and 4.4 m^{-1}, respectively, which is shown in Fig.5(a). Then, tie the soft finger with three iron sheets in turn. The soft robot is bended as three curvatures, one of which is as shown in Fig.5(b). By means of the steel tube coating, the sensors keep away from the tension of the action. On the other hand, the bending wouldn't be hindered since the steel tubes are slim and arranged along the horizontal direction. Because the elastic modulus

of soft finger is much less than the iron sheet, the curvature of the soft finger equals to that of the tied iron sheets approximately. Subsequently we test the temperature responses for different curvatures, respectively.

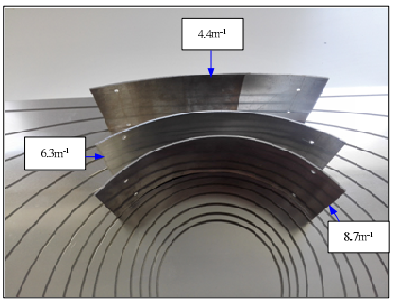

(a)

(b)

Fig.5 The method for the fixed curvature: (a) The steel plate and three iron sheets with different curvatures; (b) The prototype bend along the curvature of 6.3 m^{-1}

The experiment is implemented for 5 temperature points (15 °C, 25 °C, 35 °C, 45 °C, 55 °C) in the high-low temperature box GDW-100. The wavelengths of sensors and results of electronic thermometer are recorded for 10 min at every temperature point and every curvature, respectively. The averaged measurement temperatures of 5 FBGs for different curvatures are illustrated in Fig.6 in which the maximum standard deviation is 0.8 °C.

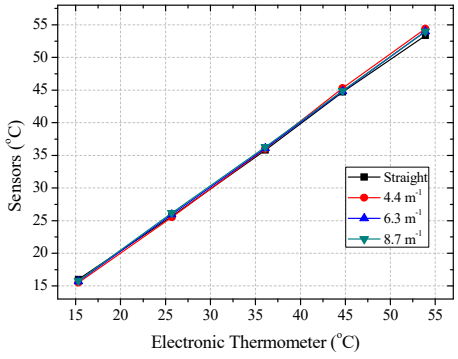

Fig.6 The averaged measurement temperatures for different curvatures in high-low temperature box

From the Fig.6, we can find the bending has little influence on the temperature coefficient of sensors. And in the working range, the sensor network has well linearity and accuracy. On the other side, considering that the figure results from four heating cycling tests, the uniformity indicates the sensor network achieves decent repeatability. Therefore the method can realize the temperature-aware function for soft robot.

In the above experiments, the entire soft finger is placed in the surrounding of the same temperature. For expressing the temperature variations along the lengthways, half finger (sensor1 and 2) is above water and another half finger (sensor3~7) is under water in this experiment. The water temperature controlled by Fluke 7381 bath is set as 10 °C, 30 °C, and 50 °C, respectively. At every temperature point, the measurements of sensors sustain 15 min at least. For demonstrating the advantage of soft finger, the three iron sheets of different curvatures are applied again. The fixed manner is similar as the previous.

For clearly showing the measured temperature of different parts, the experiment results of the sensor network are depicted by color chart. In Fig.7, the charts of the same row present at the same curvature, and the charts of the same column are at the same water temperature. We can find the bottom part has the uniform temperature in every column. The color of the top part is a little different from others because the temperature of water isn't equal to the room (20 °C). In the first row, the color of top point has least change because it is farthest away from the water. Following the curvatures become greater, the colors of top approach to the colors of the bottom.

In summary, by the above experiments, it demonstrates that the proposed sensor network which can sense the ambient temperature accurately, is little influenced by the bending and can reflect the temperature gradient of surrounding. With the merits of waterproof and anti-electromagnetic interference, the FBG temperature sensor is more promising senor for soft robot than the convention electrical thermometer.

In this paper, we present a novel technique to realize temperature perception of soft robot finger using optical fiber gratings. The technique is based on the mapping relationship between the temperature and wavelength shift of FBG. The special coating and alignment of FBG units may provide the fibers protection and avoid the influence of strain which can be caused by the finger movement and external factor. For sticking optical fiber with soft finger firmly, two kinds of adhesives are applied. Then the sensor network is calibrated in high precision bath. After calibration, the prototype is measured in the room, high-low temperature box and temperature gradient environment, respectively. The experimental results indicate that the sensor network has well linearity and accuracy, the resolution is better than 1 °C (0.1 °C in theory). Three different bending curvatures are tested in order to investigate the sensor network behavior variations

with an increase of curvature. The experiment proves that the bending of finger has little effect on the temperature measurement. This sensor network can be integrated into the soft finger in a simple, practical, and noninvasive manner and the performance of the proposed prototype meets temperature-aware requirement of soft robot.

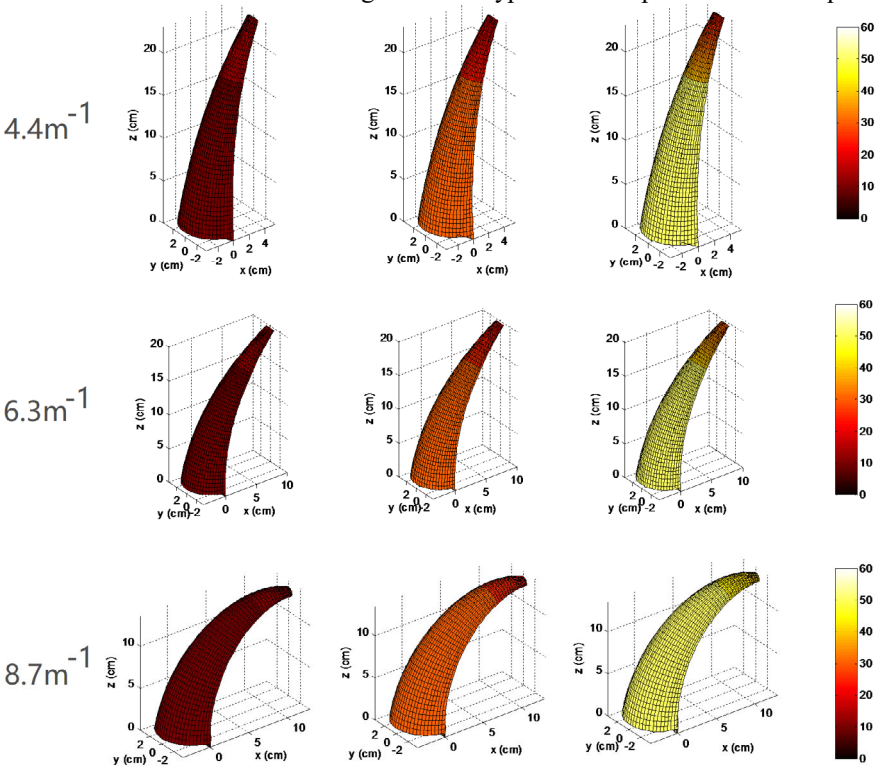

Fig.7 The experiment results of gradient measurement for different curvatures

The significance of this sensing scheme we think lies in the following aspects. Firstly, it's the first time that the FBG is employed to sense the temperature of the soft robot, which verifies its validity. This method could be suitable for other flexible occasions, like morphing wings. Secondly, it proposes a bargain solution of soft robot temperature sensor by taking advantage of the flexible nature of optical fiber. The optical fibers and opto-electronic components have high quality and low price. And optical fiber sensor has advantages of waterproof and anti-electromagnetic interference, which is superior to the electronic ones. Indeed, the reliability of the information from the sensors is the key to actuate the robot. Finally, by making good use of this ability, the soft finger can not only sense temperature but also realize more practical applications, such as liquid level and deep detection, heat source search, thermal flow velocity measurement and so on. We believe that optical fiber sensor will play a key role in the temperature-sensing of soft robotics. In the future, the sensors can be fabricated using the advanced optical fiber, such as sapphire optical fiber, for wider temperature range and higher stability.

References

[1] H. T. Wang, X. F. Peng and B. M. Lin, Journal of South China University of Technology **48**, 2 (2020). (in Chinese)

[2] A. J. Ijspeert, Science **6206**, 196 (2014).

[3] C. Laschi, M. Cianchetti, B. Mazzolai, L. Margheri, M. Follador and P. Dario, Advanced Robotics **7**, 709 (2012).

[4] J. F. Chen and X. S. Wang, Advances in Intelligent Systems and Computing **345**, 475 (2015).

[5] M. Cianchetti and T. Menciassi, Biosystems and Biorobotics **17**, 75 (2017).

[6] C. Lee, M. Kim, Y.J. Kim, N. Hong, S. Ryu, H.J. Kim and S. Kim, International Journal of Control Automation and Systems **1**, 3 (2017).

[7] D. Raffaele, T. Giacomo, B. Luca, C. Vincenzo, M. Bruno and D. Chiara, Science Robotics **3**, 1 (2017).

[8] T. Chen, M. l. Ye, S. l. Liu and Y. Deng, Optoelectronics Letters **14**, 92 (2018).

[9] J. F. Chen and X. S. Wang, Advances in Intelligent Systems and Computing **345**, 475 (2014).

[10] S. J. Rizzolo, A. Périsse, Y. Boukenter, E. Ouerdane, J. R. Marin, M. Macé, S. Cannas and S. Girard, Scientific Reports **7**, 8766 (2017).

[11] S. Li, H. Zhao and F. Robert, Mrs Bulletin **42**, 138 (2017).

[12] C. J. Yu, Fully Rubbery Stretchable Electronics, Sensors, and Smart Skins, Proceedings of SPIE **10982**, 2019.

[13] D. Rus and M. T. Tolley, Nature **521**, 467 (2015).

[14] Y. Cao, C. Zhao and Z. R. Tong, Optoelectronics Letters **11**, 438 (2015).

[15] Y. Q. Li, S. Liu and S. H. Inaki, Sensors **9**, 2084 (2017).
[16] C. Wenbin and C. Chiachung, Sensors **10**, 3073 (2010).
[17] A. Kus, Y. Isik, M. C. Cakir, S. Coşkun and K. Özdemir, Sensors **15**, 1274 (2015).
[18] M. Malits and Y. Nemirovsky, Sensors **17**, 1739 (2017).
[19] Y. H. Han, C. B. Tian, Q. H. Li and S. W. Du, Journal of Materials Chemistry C **2**, 8065 (2014).
[20] W. Zhang, X. P. Lou, M. L. Dong and L. Q. Zhu, Optoelectronics Letters **13**, 05 (2017).
[21] T. Li, L. Qiu and H. Ren, IEEE/ASME Transactions on Mechatronics **25**, 1 (2020).
[22] C. L. Zhao, The Perception Mechanism and Experiment Research of the Robot Whisker Array Based on FBG, Shandong University, 2016. (in Chinese)
[23] M. Luca, O. M. Calogero and S. Edoardo, Frontiers in Neurorobotics **13**, 8 (2019).
[24] L. G. Arnaldo, D. R. Camilo and P. J. Maria, Optics and Laser Technology **112**, 323 (2019).
[25] Q. Jiang and Q. Wei, Pressure and Bending Sensing of Soft Fingers Based on FBG, Proceedings of SPIE **11340**, 2019.
[26] J. K. Sahota, N. Gupta and D. Dhawan, Optical Engineering **59**, 6 (2020).
[27] C. Quan, L. Yang and R. Jing, Optical Engineering **58**, 7 (2019).
[28] O. Frazão, Optical Engineering **52**, 992 (2013).
[29] L. D. Lu, H. Li, Q. F. Yao, W. He and L. Q. Zhu, Optoelectronics Letters **12**, 421 (2016).
[30] Q. Zhou, T. G Ning, L. Pei, J. Li, C. Li and C. Zhang, Optoelectronics Letters **8**, 414 (2012).